18

Variable Freshwater Input to the Arctic Ocean During the Holocene: Implications for Large-Scale Ocean-Sea Ice Dynamics as Simulated by a Circulation Model

Matthias Prange and Gerrit Lohmann

Summary. Recent geological studies revealed that the freshwater input to the Arctic Ocean was highly variable during the Holocene. In the present study we examine the influence of changing Arctic freshwater runoff and low-saline Bering Strait inflow on large-scale ocean-sea ice dynamics by means of a general circulation model of the Arctic Ocean, the Nordic Seas, and the Atlantic. Discharge distributions used are based on paleohydrological reconstructions for the early (approx. 10 ka) and middle (about 7 ka) Holocene. Keeping all other forcing fields and topography at present-day values, we isolate the effect of a variable freshwater supply to the Arctic Ocean. The model experiments show that Arctic freshwater input is vitally important for the polar oceanic circulation, influencing the size of the Beaufort Gyre and the path of the Transpolar Drift. The results indicate that long-term Holocene variability in Arctic freshwater forcing had the potential to cause considerable variability in Arctic Ocean dynamics on a century-to-millennium scale. Moreover, a relatively warm Bering Strait inflow exerts a strong influence on polar sea ice. It is likely that a gradual increase in the influx during the early Holocene slowly affected the polar climate by melting some ice and decreasing the surface albedo in the eastern Arctic. The effect of Arctic freshwater forcing on the Atlantic thermohaline circulation (THC) is small in our experiments. We conclude that changes in the Arctic Ocean freshwater input alone only played a minor role for potential variations in the THC during the Holocene.

18.1 Introduction

The Arctic Ocean is unique among all oceans because its hydrographical characteristics are profoundly influenced by a large input of freshwater from the surrounding continents and from the inflow of low-saline Pacific water through Bering Strait (e.g., [1]). Relative to its size the Arctic Ocean receives the largest river water input of all oceans. Since the thermal expansion coefficient of sea water is very small at low temperatures, the density of cold polar water masses is primarily a function of salinity. Therefore, freshwater influx and ocean dynamics are closely linked in the Arctic. The Arctic freshwater budget

has gained much attention in recent climate research projects (e.g., [999]), mainly because of the following two reasons.

First, inflowing freshwater is crucial for the density stratification in the Arctic Ocean. In particular, the formation of a cold halocline depends on river runoff (e.g., [997]). The cold halocline, an isothermal near freezing-point layer located at 50–150 m depth over most parts of the Arctic basins, effectively shields the surface from heat stored at intermediate depths in the Atlantic layer. It is therefore of utmost importance for the Arctic sea ice cover, which acts as a natural refrigerator for the planet due to its high albedo.

Secondly, the freshwater surplus of the Arctic Ocean is balanced by an export of freshwater, as liquid water and sea ice, through Fram Strait and through the channels of the Canadian Archipelago (Fig. 18.1; see Fig. 18.2 for a geographical overview). Freshwater of Arctic origin is thus advected into the Labrador Sea as well as into the Nordic Seas where convective regimes of major importance to North Atlantic Deep Water (NADW) formation are located. Therefore, the Arctic freshwater budget is closely linked to the thermohaline conveyor belt [837] which, in turn, plays a major role in the global climate system (e.g., [129]).

River runoff into the Arctic Ocean is expected to increase in the future due to the rise in greenhouse gas concentrations in the atmosphere [727]. Given the importance of the Arctic freshwater budget for ocean-sea ice dynamics and, hence, for the climate system, an assessment of its long-term variability is desirable. For this purpose, it is useful to study the past.

Recent geological studies have revealed that the freshwater input to the Arctic Ocean was highly variable during the Holocene (for references see Sect. 18.2). During the Late Glacial–Holocene transition the melting of northern hemisphere ice sheets altered the hydrological balance, and runoff patterns changed dramatically (e.g., [1042], [984]). Freshwater routing by the Laurentide ice sheet during the deglaciation has been studied by Licciardi et al. [616]. Using new reconstructions of the ice sheet they found that enhanced meltwater input to the Arctic Ocean occurred only late in deglaciation. Model results from Marshall and Clarke [695] confirm these findings and show that Canadian Arctic river basins were not activated until 12 ka (12,000 calendar years before present).

During the middle Holocene variations in the freshwater budget of the Arctic Ocean were mainly caused by changes in the $P-E$ (precipitation minus evapotranspiration) pattern over Asia which governs the discharge of Siberian rivers. According to bioclimatic vegetation modelling, annual precipitation in Siberia was about 10 cm greater in the mid-Holocene than today [731]. Most of the increase was concentrated in East Siberia. Besides, a retreat of the permafrost zone was likely to have altered the Arctic freshwater balance (e.g., [1094]).

Another source in the freshwater budget of the Arctic Ocean which might have been highly variable is Pacific water flowing through Bering Strait. The strait remained closed during the last deglaciation and only reopened 12–13

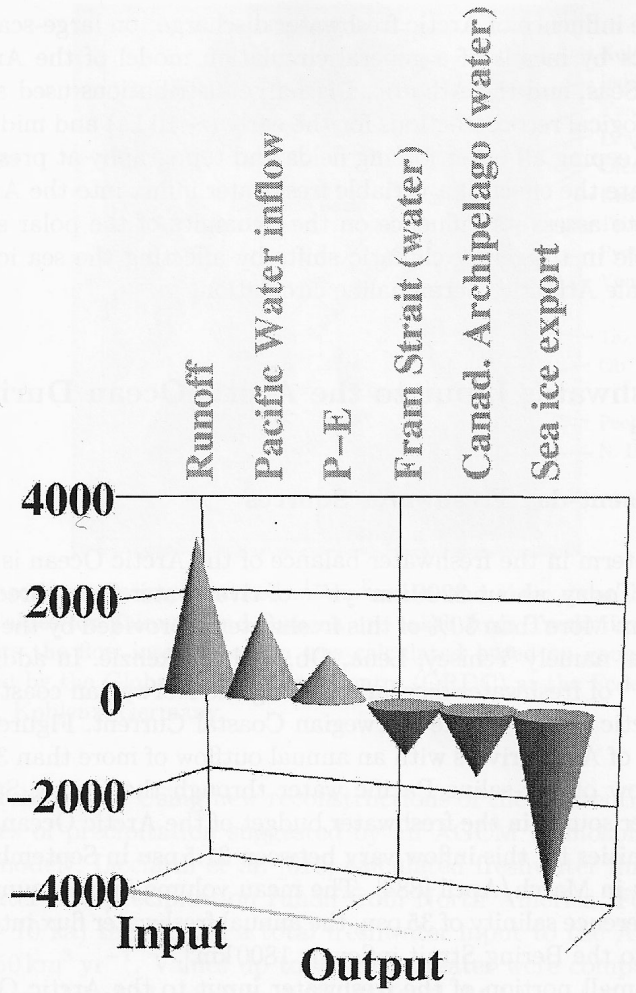

Fig. 18.1. Present-day freshwater budget of the Arctic Ocean (only the major contributors are shown). Values (in $km^3\ yr^{-1}$) are based on [1], [998], and [836]. Sea ice is mainly exported through Fram Strait. $P - E$ denotes net precipitation.

ka ago. The Bering land-bridge inundation was completed by 5–6 ka [271]. Today about 0.8 Sv (1 Sv = 1 Sverdrup = $10^6\,m^3\,s^{-1}$) of low-saline (i.e. about 32.5 psu) Pacific water is flowing northward through the strait which has a mean depth of 50–60 m [884]. It is likely that the throughflow was strongly reduced in the early Holocene due to a shallower bathymetry.

Even though geological studies have shed some light on the long-term variability of the Arctic freshwater budget, the effects on ocean circulation and sea ice cover are not known. Numerical modelling, however, may help to improve our understanding of the dynamical system. In the present study we

examine the influence of Arctic freshwater discharge[1] on large-scale ocean-sea ice dynamics by means of a general circulation model of the Arctic Ocean, the Nordic Seas, and the Atlantic. Discharge distributions used are based on paleohydrological reconstructions for the early ($\sim$ 10 ka) and middle ($\sim$ 7 ka) Holocene. Keeping all other forcing fields and topography at present-day values, we isolate the effect of a variable freshwater influx into the Arctic Ocean. The aim is to assess its influence on the dynamics of the polar seas and the potential role in triggering climatic shifts by affecting the sea ice cover and the large-scale Atlantic thermohaline circulation.

18.2 Freshwater Input to the Arctic Ocean During the Holocene

18.2.1 Present-day Freshwater Sources

The largest term in the freshwater balance of the Arctic Ocean is river runoff (Fig. 18.1). Today, about $3200\,\mathrm{km^3\,yr^{-1}}$ of river water flows directly into the Arctic Ocean. More than 50% of this freshwater is provided by the four largest Arctic rivers, namely Yenisey, Lena, Ob, and Mackenzie. In addition, about $380\,\mathrm{km^3\ yr^{-1}}$ of freshwater discharged along the Norwegian coast is advected into the Arctic Ocean by the Norwegian Coastal Current. Figure 18.2 shows the location of Arctic rivers with an annual outflow of more than $30\,\mathrm{km^3\,yr^{-1}}$.

The inflow of low-saline Pacific water through the Bering Strait constitutes another source in the freshwater budget of the Arctic Ocean (Fig. 18.1). Typical salinities for this inflow vary between 31.5 psu in September/October and 33.5 psu in March/April [884]. The mean volume flux amounts to 0.8 Sv. Taking a reference salinity of 35 psu, the annual freshwater flux into the Arctic Ocean due to the Bering Strait inflow is $1800\,\mathrm{km^3}$.

Only a small portion of the freshwater input to the Arctic Ocean is due to precipitation over the sea surface. $P - E$, i.e. net precipitation, is roughly $1000\,\mathrm{km^3\,yr^{-1}}$ [1], [836].

18.2.2 Freshwater Input During the Early Holocene ($\sim$ 10 ka)

At the beginning of the Holocene, remnants of glacial ice sheets were still present in northeastern North America and Scandinavia (e.g., [811]). Numerical reconstructions [695], [616] suggest that the waning of the Laurentide ice sheet during the last stages of the deglaciation gave rise to a considerable flux of meltwater into the Arctic Ocean. Part of this water entered the ocean via the Mackenzie River basin, another part came from the northern islands of the

[1] Here and henceforth the term "Arctic freshwater discharge" ('input', 'influx', etc.) denotes both continental runoff and Bering Strait inflow, even though the latter is not pure freshwater.

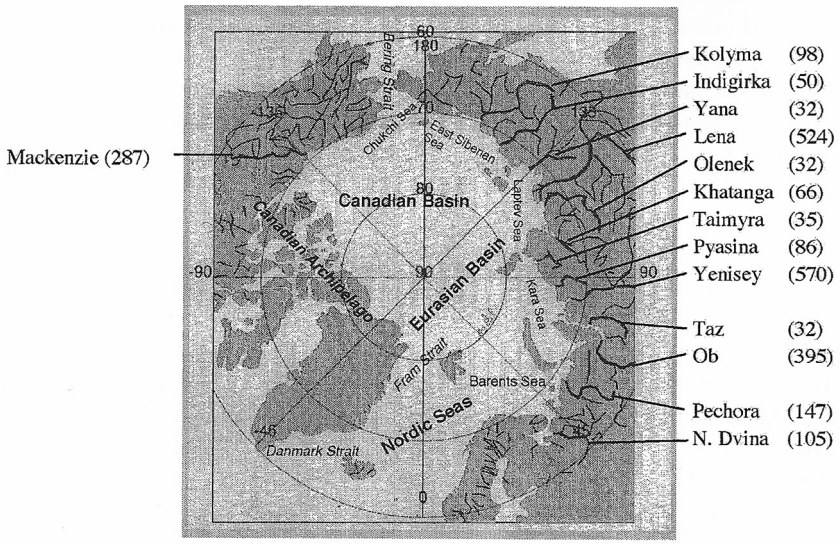

Fig. 18.2. Arctic rivers implemented in the model and their mean discharge (in $km^3\ yr^{-1}$). Values for Taimyra and Pyasina are taken from Treshnikov [1074]. For all other rivers the flow into the ocean was calculated based on gauged discharge data, provided by the Global Runoff Data Centre (GRDC) at the Federal Institute of Hydrology, Koblenz, Germany.

Canadian Archipelago. Using new reconstructions of the Laurentide ice sheet and estimates of precipitation suggested by an AGCM (atmosphere general circulation model), Licciardi et al. [616] calculated freshwater fluxes derived from meltwater and precipitation runoff from North America. For the early Holocene ($\sim$ 10 ka) they found a total freshwater input to the Arctic Ocean of about $1250\,km^3\,yr^{-1}$. Values up to 4 times greater were computed by the ice-dynamics model of Marshall and Clarke [695]. Melting of Fennoscandian ice sheet remnants provided freshwater for the Norwegian Coastal Current. It is likely that a considerable portion of this meltwater was advected into the Barents Sea.

Direct river discharge into the Barents Sea was probably higher at 10 ka than today. Sidorchuk et al. [969] reconstructed the paleohydrology of the Vychegda River from the grain size of channel deposits, paleochannel morphology, and paleolandscape features. The Vychegda River is a major contributor to the Northern Dvina. It is reasonable to assume that changes in its flow are representative for the total river runoff from the northern Russian Plain into the Barents Sea.

The variability of the paleoriver water supply to the Kara and Laptev Seas was studied by Boucsein [95]. She analyzed the distribution of freshwater alginite (chlorococcalean algae) in marine sediment cores from different locations in the Kara Sea and along the Eurasian continental margin. For $\sim$ 10 ka

the record indicates an increased freshwater input to the Kara Sea, while the freshwater supply to the Laptev Sea was probably similar to the modern one.

As to the early Holocene runoff into the East Siberian Sea, reliable data have not been published so far. The hydrography in that region is, however, more influenced by the Bering Strait inflow than by river runoff. In view of the strait's shallow depth at 10 ka [271], the inflow of Pacific water was possibly only half of the modern one.

18.2.3 Freshwater Input During the Middle Holocene ($\sim$ 7 ka)

Cheddadi et al. [158] estimated $P - E$ across Europe for the middle Holocene from pollen data using the modern pollen analogue technique constrained with lake-level data. Their results suggest that $P - E$ over Norway was 5–25 cm yr^{-1} less than at present, while $P - E$ was 10–15 cm yr^{-1} greater in eastern Europe. According to these results, river runoff into the Norwegian Sea was smaller than now, whereas freshwater discharge into the Barents Sea was somewhat higher.

The distribution of chlorococcalean algae in marine sediment cores indicates that mid-Holocene freshwater input to the Kara Sea was slightly lower than at present [95], while runoff into the Laptev Sea was much larger, maybe twice as high as today [568]. This extreme river discharge is consistent with strongly increased precipitation in Yakutia reconstructed by Monserud et al. [731].

As to the freshwater discharge from the East Siberian and North American coasts, we refer to reconstructions by Belyaev and Georgiadi [64]. Utilizing paleofloristic data and climatic indicators, they estimated spatial patterns of runoff. The results suggest larger freshwater input to the East Siberian Sea, and North American runoff close to the present one.

18.3 Model Design and Experimental Set-up

18.3.1 Ocean-Sea Ice Model and Forcing

In order to examine the effects of freshwater discharge on high-latitude ocean dynamics, we utilize a coupled ocean-sea ice model. The ocean model is set up on the base of the hydrostatic Geophysical Fluid Dynamics Laboratory (GFDL) primitive equation model MOM-2 [789], employing the implicit free-surface method by Dukowicz and Smith [259]. The model domain spans the Arctic Mediterranean (i.e. the Arctic Ocean proper and the Nordic Seas) and the Atlantic Ocean north of approximately 20°S. The model is formulated on a rotated grid to avoid the singularity of geographical coordinates at the pole (Fig. 18.3). It has a horizontal resolution of about 100 km and 19 non-equidistant levels in the vertical. Using the flux-corrected transport (FCT) algorithm for tracer advection, explicit diffusion is set to zero [367].

The ocean model is coupled to a dynamic-thermodynamic sea ice model with viscous-plastic rheology, which is defined on the same horizontal grid [429]. We emphasize that the ocean-sea ice model is fully prognostic, i.e. no diagnostic or restoring terms are added to the conservation equations. A detailed description of the model can be found in [836].

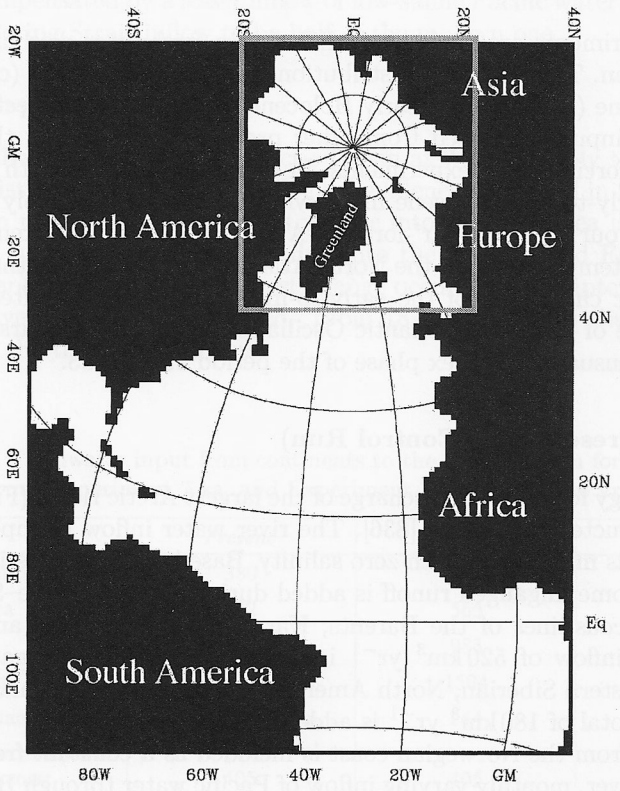

Fig. 18.3. Domain of the model. The model equations are defined on a rotated grid. Both the geographical and the model grid coordinates are displayed. The frame marks the area that is shown in Figs. 18.4–18.8.

The ocean-sea ice model is forced by atmospheric fields, comprising 2 m-temperature, 2 m-dewpoint temperature, cloud cover, precipitation, wind speed, and wind stress. Except for daily wind stress, all forcing fields are monthly varying. The atmospheric fields are derived from a validated 15 year (1979–1993) set of assimilated data provided by the reanalysis project of the European Center for Medium-Range Weather Forecasts (ECMWF). The data have been processed to construct a 'typical' year, i.e. a mean annual cycle with daily fluctuations superimposed [898]. In addition to atmospheric forcing, the ocean-sea ice system is forced by river runoff and Bering Strait inflow.

Fourteen Arctic rivers (Fig. 18.2) are implemented as well as some additional ungauged runoff from the Arctic coastlines (see below). For the Atlantic portion of the model domain, the eight largest rivers are included as well as the freshwater supply from Hudson Bay and the Baltic Sea.

18.3.2 Experiments

Three experiments are performed, differing in freshwater discharge into the Arctic Ocean. The discharge distributions refer to present-day (control run), mid-Holocene ($\sim$ 7 ka), and early Holocene ($\sim$ 10 ka). The effect of variable freshwater input is isolated from other processes by applying the same atmospheric forcing in all experiments. In this context, it is worth noting that the real early-to-mid Holocene mean wind forcing was probably not too far away from our 'typical year'-forcing. A recent analysis of alkenone-derived sea surface temperatures in the North Atlantic realm indicates that the mean atmospheric circulation of the early-to-mid Holocene was shifted to a high index phase of the North Atlantic Oscillation [877], which bears similarities with the unusual high index phase of the period 1979–1993.

18.3.2.1 Present-day (Control Run)

A climatology for monthly discharge of the largest Arctic rivers (Fig. 18.2) has been constructed by Prange [836]. The river water inflow is implemented in the model as mass fluxes with zero salinity. Based on various estimates (e.g., [831], [2]) some ungauged runoff is added during summer (June–September). Along the coastlines of the Barents, Kara, and Laptev Seas an additional freshwater inflow of $520\,\mathrm{km}^3\ \mathrm{yr}^{-1}$ is equally distributed. Ungauged runoff from the eastern Siberian, North American and northern Greenland coasts is smaller: a total of $180\,\mathrm{km}^3\ \mathrm{yr}^{-1}$ is added in these regions.

Runoff from the Norwegian coast is included as a constant freshwater inflow. Moreover, monthly varying inflow of Pacific water through Bering Strait is implemented based on direct measurements (see Sect. 18.2.1). Aside from being a source term in the Arctic Ocean freshwater budget, the Bering Strait inflow is associated with a heat supply during the summer months. The temperature rises up to 4°C in September, while winter temperatures (December–May) are at freezing for the salinity [60], [884].

18.3.2.2 Experiment 10 ka

Even though there is geological evidence for increased freshwater runoff from the continents into the Arctic Ocean at the early Holocene, a quantification is difficult and subject to considerable uncertainty. Based on geological studies, summarized in Sect. 18.2.2, we estimate the 10 ka freshwater discharge to force the Arctic Ocean. We presume river water inflow from the Norwegian

coast as well as into the Barents and Kara Seas to be 25% higher than today. Extreme runoff, amounting to three times the modern one, is assumed from North American and northern Greenland coasts. To implement these changes in the ocean model, we increase the freshwater input to each coastal grid cell by the respective percentage.

Concerning the freshwater budget of the Arctic Ocean, the enhanced runoff is partly compensated by a lesser inflow of low-saline Pacific water. We assume the 10 ka Bering Strait inflow to be half of the modern one.

18.3.2.3 Experiment 7 ka

For the freshwater forcing of the Arctic Ocean at 7 ka we apply the following discharge distribution, based on geological evidence presented in Sect. 18.2.3. Runoff from the Norwegian coast as well as into the Kara Sea is 25% lower than today, whereas the freshwater flux into the Barents and East Siberian Seas is enhanced by 25%. The largest change occurs in the Laptev Sea. Here, the total river discharge is doubled. Table 18.1 summarizes the freshwater forcings for the three experiments.

Table 18.1. Freshwater input from continents to the Arctic Ocean for the present-day control run, Experiment 7 ka, and Experiment 10 ka. Units are $km^3\ yr^{-1}$.

Region	*Present*	*7 ka*	*10 ka*
Norwegian coast	380	285	475
Barents Sea	452	565	565
Kara Sea	1310	983	1638
Laptev Sea	797	1594	797
East Siberian Sea	195	244	195
North American/North Greenland coast	405	405	1215
Total	**3539**	**4076**	**4885**

18.4 Results

For a direct comparison of the results, the three experiments are started from the same initial conditions. The initial state is taken from a spin-up run described by Prange [836]. For each experiment the model is integrated 60 years. This time span corresponds to about 6 times the mean residence time of present-day Arctic halocline waters [938] and is long enough for anomalous Arctic freshwater input to affect the large-scale Atlantic thermohaline circulation [366], [837].

18.4.1 Upper Ocean Circulation and Sea Ice Cover in the Arctic Mediterranean

18.4.1.1 Present-day (Control Run)

The control run is aimed at simulating the present-day circulation. In the following, we show annual mean fields which apply to the last year of the integration period[2].

The ocean circulation averaged over the top 80 m in the polar and subpolar seas[3] is presented in Fig. 18.4a. The model captures the characteristic features of the observed flow pattern markedly well. A strong cyclonic gyre dominates the Nordic Seas, consisting of the EGC (East Greenland Current) in the west, and the NAC (Norwegian Atlantic Current) in the east. The latter transports warm and salty water from the Atlantic to the North, while the EGC carries cold, relatively fresh polar water to the South, where it leaves the Nordic Seas through Denmark Strait. Atlantic water enters the Barents Sea, bringing some heat into the Arctic Ocean. This current constitutes the southern branch of an overall cyclonic flow pattern in the eastern Arctic Ocean. The Canadian Basin in the western Arctic is dominated by the anticyclonic Beaufort Gyre. The western anticyclonic gyre meets the eastern cyclonic circulation in the central Arctic, thereby forming the current system of the Transpolar Drift (TPD). The TPD carries polar waters towards the outlets of the Arctic Ocean, namely Fram Strait and Nares Strait (Canadian Archipelago).

Near-surface salinities are shown in Fig. 18.4b. High salinities (> 35 psu) in the Norwegian and the western Barents Seas indicate the inflow of Atlantic waters from the South. In the Arctic Ocean proper, salinities are much lower with minima in the Siberian shelf seas due to inflowing river water. Low-saline shelf waters are advected into the central Arctic Ocean, eventually leaving the Arctic Ocean through Fram Strait or the Canadian Archipelago. The southward flow of polar water in the EGC causes low salinities in the western Nordic Seas.

The distribution of sea ice is presented in Fig. 18.5. We recognize a typical pattern that is well-known from other model studies (e.g., [456], [429]) and which is consistent with sonar data (e.g., [456], [96]). This pattern is characterized by maximum ice thickness north of Canada, an ice thickness of 3–4 m near the pole, and relatively thin ice to the north of Siberia. The mean ice drift is indicated by arrows in Fig. 18.5. It resembles the upper ocean circulation, with an anticyclonic gyre over the Canadian Basin, a TPD, outflow through Fram Strait, and an EGC.

[2] Multi-year averaging is not necessary, since internal interannual variability proves to be negligible in the modelled Arctic Ocean.

[3] The top 80 m are represented by the three topmost levels of the model grid and comprise the surface mixed layer with the upper part of the cold halocline in the Arctic Ocean.

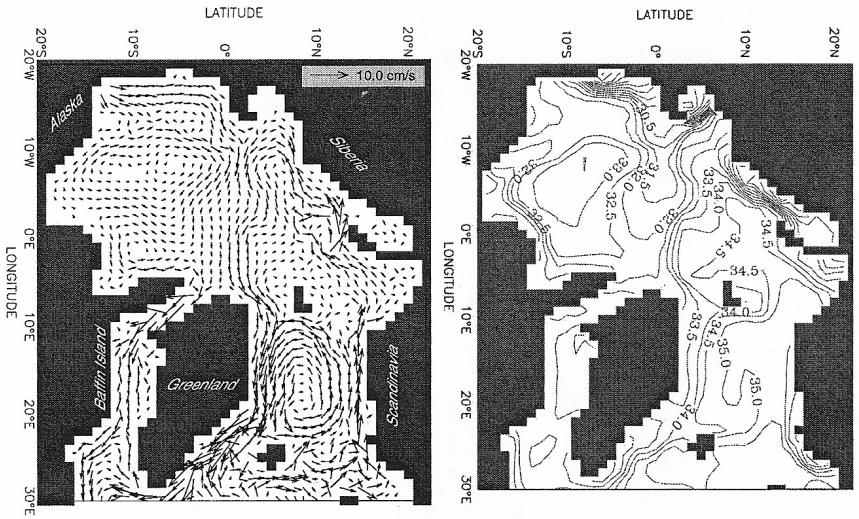

Fig. 18.4. Annual mean fields of the upper Arctic Ocean (averaged over 0–80 m) in the present-day control run: (**a**) Velocity, (**b**) salinity (contour interval is 0.5 psu). Labels refer to the rotated model grid.

18.4.1.2 Experiment 10 ka

The freshwater forcing of Experiment 10 ka is described in Sect. 18.3.2.2. Strongest differences relative to the present-day forcing consist of a huge freshwater influx from the North American/Greenland coasts and a reduced inflow of Pacific water through Bering Strait. These changes are directly reflected in the field of upper ocean salinity. Fig. 18.6a shows that freshwater from the Canadian coast is advected by the Beaufort Gyre into the central Arctic. Since the Bering Strait inflow is reduced, part of this freshwater can readily enter the Chukchi and East Siberian Seas. Lowered surface salinities in the Kara, Barents, and Norwegian Seas are directly caused by enhanced local runoff (see Table 18.1). The eye-catching high-salinity tongue north of Greenland (Fig. 18.6a) results from the reduced inflow of low-saline Pacific water and a changed circulation pattern.

Figure 18.6b shows differences in upper ocean velocity relative to the control run. Over the Canadian Basin and the East Siberian Sea the anticyclonic pattern is intensified. A cyclonic gyre north of Greenland and changes in the Eurasian Basin result in a modified path of the TPD. The reduced Bering Strait inflow is compensated by a weaker outflow through the Canadian Archipelago[4] and an increased inflow via the Barents Sea, maintaining a steady Arctic Ocean mass balance.

[4] According to Zreda et al. [1200] Nares Strait was just open at 10 ka after being blocked by ice sheets during the last glaciation.

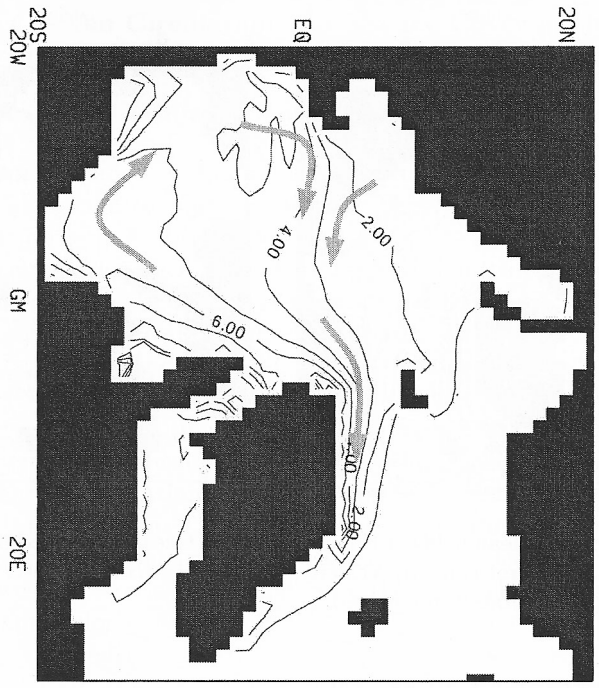

Fig. 18.5. Annual mean sea ice thickness in the present-day control run. The contour interval is 1 m. The mean ice drift pattern is indicated by arrows. Labels refer to the rotated model grid.

Differences in sea ice thickness are striking. Figure 18.7 presents annual mean differences between Experiment 10 ka and the control run. The decreased heat input due to a reduced Bering Strait inflow in Experiment 10 ka causes sea ice to be thicker by up to 1 m in the vicinity of the strait. Sea ice thickness is advected into the central Arctic. In conjunction with lowered heat fluxes from the ocean (not shown) owing to a stronger salinity stratification, this results in a thicker ice cover over wide areas of the Arctic Ocean. The drift of sea ice is coupled with ocean currents through ocean-sea ice stresses. Therefore, differences in sea ice motion between Experiment 10 ka and the control run are almost identical to differences in the upper ocean circulation (Fig. 18.6b).

18.4.1.3 Experiment 7 ka

The freshwater forcing of Experiment 7 ka is described in Sect. 18.3.2.3. The most notable feature is a massive river input to the Laptev Sea. This freshwater supply is conspicuous in upper ocean salinity (Fig. 18.8a). A zone of relatively low salinity extends from the Laptev Sea to Fram Strait and beyond. Salinities lower than today appear in the East Siberian Sea due to

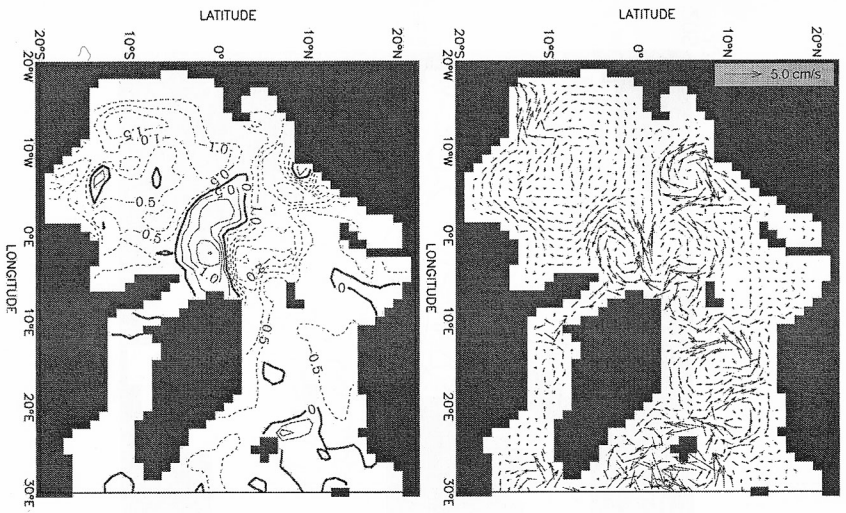

Fig. 18.6. Differences in mean upper ocean fields (averaged over 0–80 m) between Experiment 10 ka and the present-day control run (i.e., 10 ka–present-day): (**a**) salinity (contour interval is 0.5 psu), (**b**) velocity.

enhanced local runoff, whereas a smaller local freshwater inflow gives rise to higher salinities in the Kara Sea.

Changes in surface salinity are associated with changes in upper ocean velocity. Fig. 18.8b reveals considerable differences compared to the control run, particularly in the Eurasian Basin and the EGC. We find an increased throughflow in the western Fram Strait, and weaker flow through the Canadian Archipelago. The freshening of the EGC, visible in Fig. 18.8a, is associated with a stronger surface current. Thus it appears that the EGC is, at least partially, driven by freshwater-induced density gradients (cf. [1121]).

Differences in sea ice thickness between Experiment 7 ka and the control run are small, exceeding 10 cm only in few areas (not shown).

18.4.2 Meridional Overturning in the Atlantic Ocean

The zonal integral of the oceanic flow gives the meridional overturning circulation (MOC). The MOC is closely linked to the thermohaline circulation (THC) and has a well-known impact on climate (e.g., [129]). Important 'headwaters' of the THC are formed by convection in the Arctic Mediterranean. Therefore, it is commonly believed that the strength of the THC is sensitive to changes in polar and subpolar hydrography and ocean dynamics.

To assess the influence of variable Arctic freshwater input on the THC, we calculate 5-year-means of the Atlantic meridional overturning streamfunction from the end of the integration periods of the three experiments. The results are shown in Fig. 18.9. In the northern North Atlantic the modelled present-day MOC transports about 8 Sv of NADW southward at depths between 1000

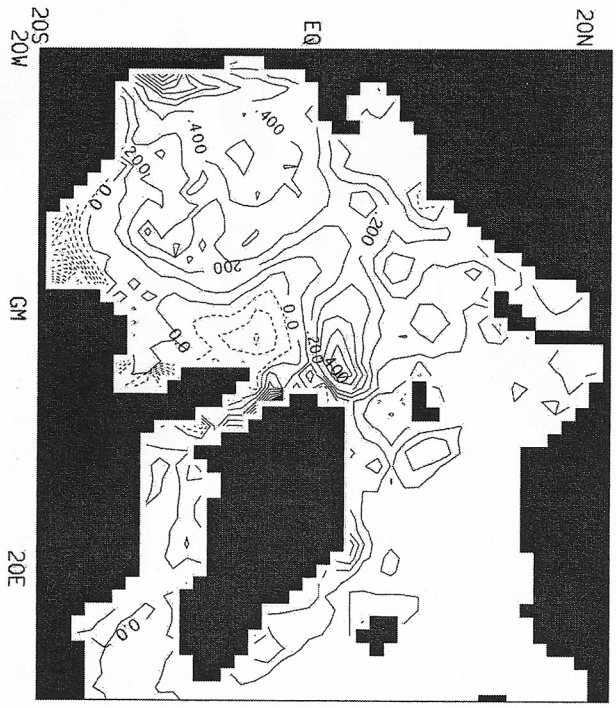

Fig. 18.7. Difference in mean sea ice thickness between Experiment 10 ka and the present-day control run. The contour interval is 0.1 m.

and 3000 m (Fig. 18.9a). Different freshwater forcings in the Experiments 10 ka and 7 ka do not result in major changes (Fig. 18.9b,c). Holocene variations of the total Arctic freshwater input appear to be too small to exert a noticeable influence on the Atlantic THC as they hardly affect the important convective regions in the Norwegian, Barents and Greenland Seas (not shown).

18.5 Towards a Dynamical Interpretation of Geological Records from the Arctic Ocean

Geological records indicate that the basic features of today's Arctic Ocean circulation have been existent throughout the Holocene: inflowing Atlantic water through Fram Strait and the Barents Sea (e.g., [654], [1001], [95]), a Transpolar Drift (e.g., [264], [62]), and an anticyclonic gyre in the western Arctic (e.g., [62]). But there are also geological evidences for variations in the strength of the currents and their hydrographic properties. Moreover, shifts in their positions seem to have occurred.

Based on heavy-mineral distributions in Arctic Ocean sediment cores, Behrends [62] reconstructed paleo-sea ice drift patterns. The data indicate

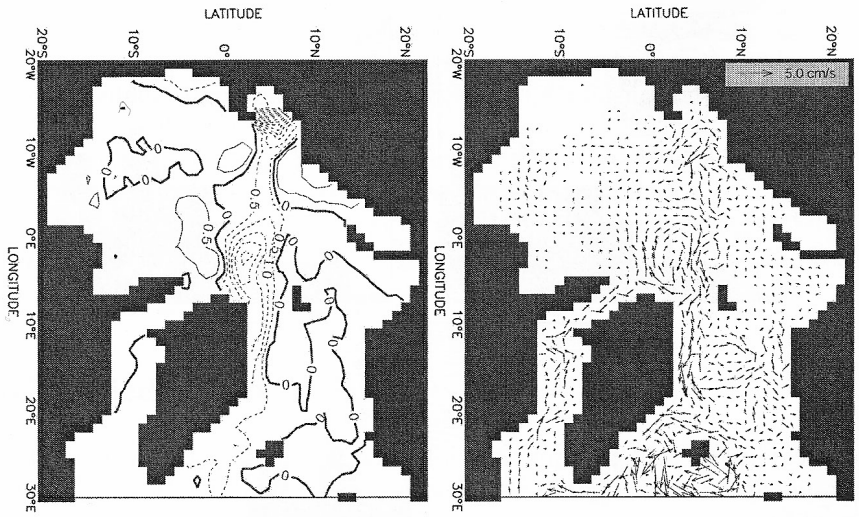

Fig. 18.8. Differences in mean upper ocean fields (averaged over 0–80 m) between Experiment 7 ka and the present-day control run (i.e., 7 ka–present-day): (**a**) Salinity (contour interval is 0.5 psu), (**b**) velocity.

that the Beaufort Gyre expanded during the early Holocene. The results from Experiment 10 ka (Fig. 18.6b) suggest that Arctic freshwater forcing, in particular the inflow of low-saline Pacific water through Bering Strait, had a substantial influence on the strength and size of the Beaufort Gyre.

Variations in the Transpolar Drift during the Holocene were hypothesized by Dyke et al. [264] from radiometric analyses of driftwood collected in the Canadian Archipelago. For the mid-Holocene, coincident with the large freshwater input to the Laptev Sea (see Sect. 18.2.3), the driftwood record suggests an eastward shift of the TPD and increased outflow through Fram Strait. The model results (Fig. 18.8b) reveal a strong connection between Arctic river runoff and the ocean circulation which may help to explain the TPD's variability during the Holocene.

18.6 Conclusions

Compiling data and information from the available literature, we tried to paint a consistent picture of freshwater influx into the Arctic Ocean for the early and middle Holocene. A quantification, however, is difficult and subject to considerable uncertainty. In the future, we expect to gain more insight into the past Arctic freshwater budget by utilizing coupled climate models. Recent efforts in paleoclimate modelling intercomparison, however, revealed considerable discrepancies among the various models in use concerning mid-Holocene $P - E$ in high latitudes (cf. [234]).

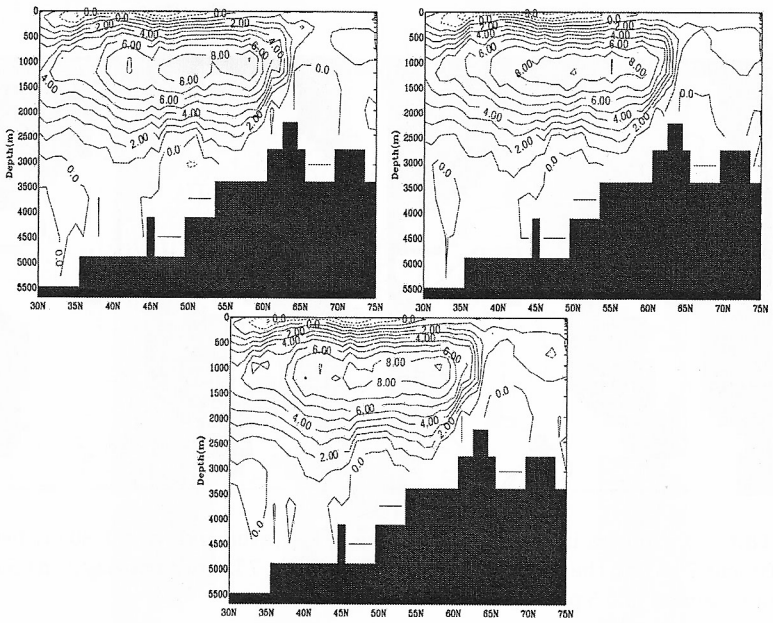

Fig. 18.9. Meridional overturning streamfunction in the North Atlantic averaged over the last 5 years of the integration period: (**a**) Present-day control run, (**b**) Experiment 10 ka, (**c**) Experiment 7 ka. The contour intervals are 1 Sv. Positive values represent clockwise rotation in the plane of the figure. Labels refer to the geographical grid.

Even though some speculative assumptions were necessary in order to construct the freshwater forcing used in our experiments, we believe that the rough magnitudes are realistic. Our results show that important effects on the polar oceanic circulation are associated with these magnitudes. The Arctic Ocean surface circulation is not simply driven by winds, as it is often claimed. Freshwater is dispersed by the oceanic flow field in upper layers, while the freshwater distribution is vitally important for driving the circulation. The results suggest that long-term Holocene variability in Arctic freshwater forcing caused considerable variability in Arctic Ocean dynamics on a century-to-millennium time scale.

A gradual deepening of the Bering Strait until the mid-Holocene was probably associated with an increasing heat flux into the Arctic Ocean. The model shows that the inflowing heat exerts a strong influence on polar sea ice. An intensified warm Bering Strait inflow causes a decline in sea ice coverage in the Chukchi and East Siberian Seas. Where sea ice is replaced by open water, the surface albedo decreases. It is therefore likely, that the gradually increasing influx of Pacific water during the early Holocene slowly affected the polar climate. Regarding the global impact of variable Arctic freshwater forcing on the oceanic circulation, the model results suggest only a small effect. Even

though the freshwater influx applied in our experiments can be considered as extreme (massive freshwater input from the North American/Greenland coasts, doubled runoff into the Laptev Sea), the influence on the strength of the THC is negligible.

In the present work, we studied the influence of Arctic freshwater forcing on the coupled ocean-sea ice system. Examining the dynamical impact of varying atmospheric forcing and ocean bottom topography, acting both separately and in concert, would be the logical next step towards understanding the role of the Arctic Ocean in Holocene climate variability.

Acknowledgments

We thank R. Gerdes and K. Herterich for their support. The careful reviews of J.-H. Kim, D. Handorf and H. von Storch helped to improve the manuscript. We kindly acknowledge financial support from the German Federal Ministry for Education, Science and Research (BMBF) through the KIHZ and DEKLIM projects.